Non-inductive Plasma Current Start-up Experiments in the TST-2 Spherical Tokamak

A. Ejiri 1), H. Kurashina 1), Y. Takase 1), K. Hanashima 1), T. Sakamoto 1), O. Watanabe 1), Y. Nagashima 1), T. Yamaguchi 1), B. I. An 1), H. Kobayashi 1), H. Hayashi 1), K. Yamada 1), H. Kakuda 1), J. Hiratsuka 1), T. Wakatsuki 1) and M. Goto 2)

1) The University of Tokyo, Kashiwa 277-8561 Japan
2) National Institute for Fusion Science, Toki 509-5292 Japan

E-mail contact of main author: ejiri@k.u-tokyo.ac.jp

Abstract. Non-inductive plasma start-up experiments have been performed on the TST-2 spherical tokamak (ST) device using ECH (2.45 GHz/ 5kW) and RF (200 MHz/ 200 kW). The RF frequency is in the lower hybrid wave frequency range. We used two types of RF antenna: a single strap loop antenna and a combline antenna to launch the RF wave. It was demonstrated that the plasma current can be started-up (after initial pre-ionization by ECH) and an ST configuration with a plasma current of about 1 kA can be formed by both types of the RF antenna. Although sustained current does not depend on the heating scenarios (ECH, RF/single-strap, RF/comb-line), equilibrium analysis revealed that two types of configuration were formed. One has a center peaked current density profile and the other has a peak near the outboard boundary. With ECH, both types can be obtained depending on the filling pressure. On the other hand, the RF/single strap scenario requires much higher filling pressure to overcome strong density pump out, and an outboard peaked current density profile was obtained as a result. The RF/combline scenario shows moderate density pump out, and a center peaked current density profile was obtained for co-drive case. In the counter-drive case, large current modulation was observed. This asymmetry indicates a directive RF current drive by the combline antenna.

1. Introduction

Key issues in spherical tokamak (ST) research are plasma current I_p start-up and the formation of the ST configuration without the use of a central solenoid (ohmic coil). Several scenarios have been studied, such as utilization of the inductive field by external poloidal field coils [1], helicity injection [2, 3] and current injection by a hot cathode [4] or by plasma guns [5]. In the RF injection scenario, RF power (usually in the EC frequency range) is injected into a configuration with a toroidal field and a weak vertical field. Successful current generation, ST formation and sustainment have been achieved. This scenario was developed in CDX-U using EC waves [6, 7], and similar experiments were performed in the ST devices: LATE [8–11], TST-2@K [12], CPD [13], TST-2 [14], MAST [15], and QUEST. A clear transition from open field line configuration to ST configuration, accompanied by a rapid increase in I_p (so-called current jump), was found in LATE. This phenomenon was also observed in other devices. In TST-2, it was demonstrated that not only EC wave, but also low frequency RF wave (21 MHz, which is high harmonic fast wave) can induce the current jump and can sustain an ST configuration [16, 17]. However, EC wave was necessary to generate the initial small current. Moreover, strong MHD activities often terminate the discharge. In order to expand the operational flexibility and to understand the mechanism of the spontaneous formation and the sustainment of ST configuration, we have installed a 200 MHz RF source in TST-2, and injected the RF wave (in the lower hybrid wave region) using two types of antenna. One is a two strap loop antenna, which was formerly used to launch the low frequency RF (21 MHz) wave. Note that only one of the two straps was used in the present experiments. The other is a combline antenna, by which travelling wave can be excited [18].

Equilibrium configuration is one of basic information to characterize tokamak plasmas. Especially in non-inductive start-up experiments, the equilibrium configuration is important to understand the current formation and sustainment mechanisms. In the pioneering experiments in CDX-U, spontaneous formation of an ST configuration was found using EC waves. It was reported that most of the plasma current flows inside the last closed flux surface [6]. On the other hand, in TST-2@K, it was found that a significant fraction (about 3/4) of the current flows in the outboard open field line region [12]. In later, both large and small fraction cases were found in TST-2 [17], but the key-parameter to control the differences were not clarified. In this paper, equilibrium analysis was performed to reveal the similarity and difference of the sustained configurations obtained by different operational scenarios. In section 2, various configurations are shown, and it was suggested that heating and fueling profile determines the difference of the configurations. In section 3, dependence of the plasma current on the external vertical field strength is shown. Finally, conclusions are presented in section 4.

2. Comparison of different heating scenarios

Firstly, EC wave sustained discharges with high and low filling pressure are compared. Secondly, an RF/single-strap wave sustained discharge is shown. Thirdly, RF/combline wave sustained discharges with opposite external field directions are compared to see the effect of the directive current drive by the combline antenna.

In order to take into account finite current density and pressure gradient in the open field line region, a truncated equilibrium [12] is used in this paper. The detail of the method was described in [17].

2.1. EC wave sustained discharge

Figure 1 shows the discharge waveforms and reconstructed profiles: one with low filling pressure (D_2/4.5 x 10^{-5} Torr) and the other with high filling pressure (D_2/1.8 x 10^{-4} Torr). As in other EC start-up experiments, a stationary external vertical field with positive curvature index was applied, which are believed to confine electrons (by mirror trapping). At the initial current formation phase, the plasma current increases gradually. The dependence of the current ramp up rate is reported in [14], and the filling pressure is one of the key-parameters to determine the rate. In the low filling pressure case, the rate is high. A current jump occurs when the initial current reaches a value proportional to the external vertical field B_Z strength [14]. In the high filling pressure discharge, the current jump was delayed. After a current jump, the current was sustained till the end of EC wave injection. The value of the sustained current is mainly determined by B_Z and dependence on other parameters is weak. The line averaged electron density for the low filling pressure is close to the O-mode cutoff density (0.07 x 10^{18} m^{-3}) for the EC wave, while the density is about twice the cutoff density for the high filling pressure case. Therefore, it is expected that the injected EC rays would experience significant refraction and/or reflection (e.g. FIG. 7 in [12]), and the resultant deposition profile may be significantly different for those two cases.

Equilibrium reconstructed profiles at t = 80 ms for the low filling pressure discharge and at t = 90 ms for the high filling pressure discharge are shown in FIG. 1 (e)-(l). The low filling pressure case is characterized by a center peaked current density and pressure profiles, while the high filling pressure case is characterized by a outboard peaked current density profile and by outboard steep pressure gradient in the open field line region. In addition to the difference

in the current density, the inboard B_Z for the former is deeply reversed from the initial external B_Z, while in the latter case, B_Z is weak and a null point often appears near the inboard boundary. This difference in the inboard B_Z can be attributed to the location of the current density peak, which is far from the inboard region in the weak B_Z case. The negative current density at the inboard region also contributes to the weak B_Z. These differences can be interpreted by the different energy deposition as follows. In the low filling pressure case, the density is low and the EC wave can access the core region, while in the high filling pressure case, the density is high and wave is presumably reflected at the outboard steep density gradient. As a result, energy is deposited at the open field line region, where perpendicularly accelerated electrons are confined due to the mirror effect. Once the pressure gradient (and density gradient) is formed at the outboard boundary region, pressure gradient current flows and the pressure and the current density profile are sustained.

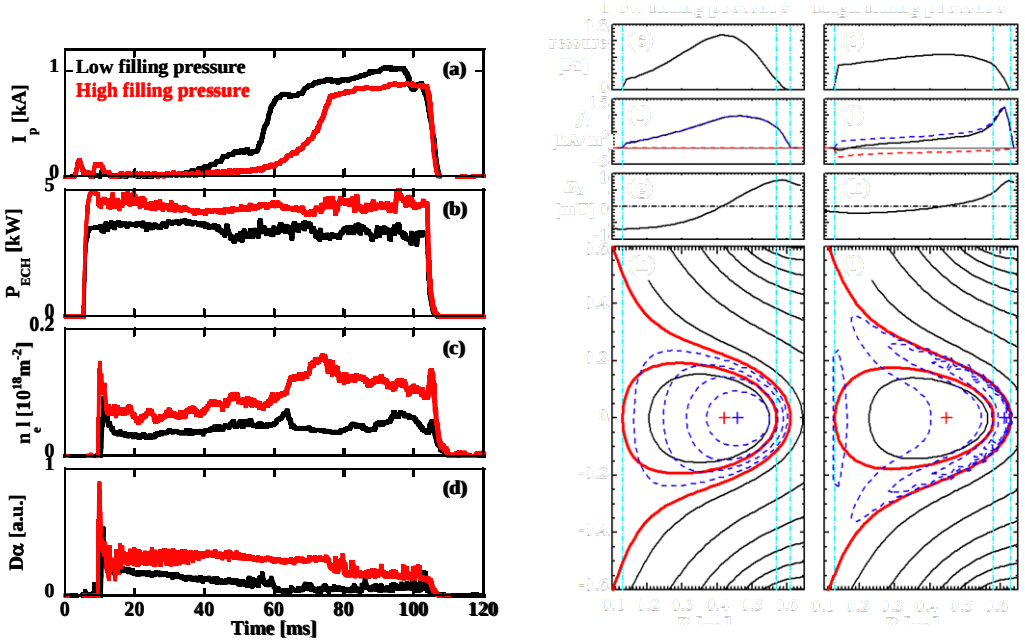

FIG. 1. Time evolution of two discharges with low ($4.5x10^{-5}$ Torr) and high ($1.8x10^{-4}$ Torr) filling pressure. Plasma current I_p (a), EC power (b), and (c), line integrated density $n_e l$ (at $Z = 0$ m, $l \sim 1$ m) (c) and $D\alpha$ emission (d). Reconstructed pressure profile (e), (i), current density profile j_t (f), (j), B_Z, profile (g), (k) and flux surfaces (h), (l) for the high and the low filling pressure discharges at $t = 80$ ms and $t = 90$ ms, respectively. In addition to the flux surface, contours of the current density (dashed curves) are also plotted. The thick contours indicate the flux surface which just touches the inboard and the outboard limiter at $Z = 0$.

2.2. RF/single-strap wave sustained discharge

For the frequency of 200 MH, only lower hybrid (LH) wave can propagate in the present plasma ($n_e \sim 10^{17}$ m^{-3}, B ~ 0.1 T). The single strap antenna can excite waves with a relatively low $n_{||}$ of the order of 1 at the antenna surface. Note that the poloidal field is about two orders of magnitude weaker than the toroidal field, so that the parallel direction almost coincides with the toroidal direction. Assuming that $n_{||}R$ is conserved due to the toroidal symmetry, the low $n_{||}$ wave cannot propagate in the outboard region and the wave is evanescent. On the other hand, the combline antenna can excite waves with a higher $n_{||}$ of around 6 at the antenna

surface, and the wave can penetrate through the plasma. In addition to the propagation, we should consider whether LH waves can be excited by the present antenna, which mainly excite fast waves with poloidal electric field and toroidal magnetic field. Although whether LH wave is excited or not is unknown, experimental results indicate that the plasma can be generated and current and an ST configuration can be formed. This issue is not discussed further in this paper.

Figure 2 shows the discharge waveforms and reconstructed profiles. In this case, initial ECH is used for the pre-ionization. The RF wave with a net power of about 30 kW was injected using one of two straps. As in the case of ECH start-up experiments, the plasma current increases gradually, and a current jump occurred and an ST configuration was sustained. The electron density and the equilibrium configuration are similar to those in the ECH high filling pressure case (see FIG. 1 (c), (i)-(l)). This is partly because of the high filling pressure (D_2/2x10^{-4} Torr). When we reduce the filling pressure, we cannot sustain the discharge. The RF power causes a strong density pump out. When we superpose a short period RF power to an EC sustained ST configuration, the electron density decreases rapidly, and the discharge were terminated unless we added gas puffing. This strong density pump out effect is observed only in this heating scenario. For the RF/combline scenario described in Sec. 2.3, we observed much more moderate density pump out. Since LH wave accelerates parallel velocity through Landau damping, if the RF power is deposited at the outboard open field line region, the RF power would evacuate electrons from the region, because those parallel accelerated electrons cannot be confined by the mirror effect. Recalling that the single strap antenna excites low $n_{\parallel}$ wave, the strong density pump out and the equilibrium configuration are qualitatively consistent with the parallel electron heating near the outboard boundary.

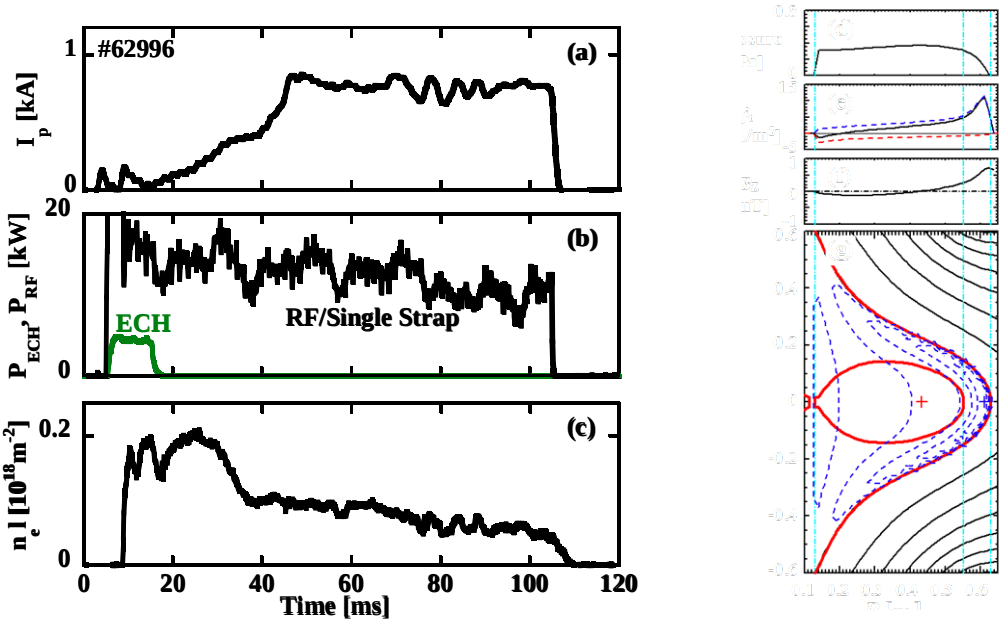

FIG. 2. Time evolution of the RF/single-strap started-up discharge. Plasma current I_p (a), EC power (b), and line integrated density (c). Reconstructed pressure profile (d), current density profile j_t (e), B_Z, profile (f) and flux surfaces (g) at t = 90 ms. In addition to the flux surface, contours of the current density (dashed curves) are also plotted. The thick contours indicate the flux surface which just touches the inboard and the outboard limiter at Z=0.

2.3. RF/comb-line wave sustained discharge

While the direction of the pressure driven current (such as the bootstrap current and Pfirsch-Schlüter current) depends on the direction of the poloidal field, the direction of the LH wave current drive is determined by the antenna structure and operating condition. With the combline antenna installed in TST-2, excitation of directive LH wave is expected [18]. In order to clarify such wave induced current drive effect, experiments with different external vertical field directions were performed. When the directions of pressure induced drive and wave induced current drive are parallel (black curves in FIG. 3 (a)-(d)), a stable ST configuration (FIG. 3 (e)-(h)) similar to the low filling pressure ECH case (see FIG. 1 (e)-(h)) was obtained. When the directions are anti-parallel, however, the ST configuration was unstable and large current modulation was observed (FIG. 3 (a)). The direction of the current itself varies when the direction of the external vertical field flips, although the direction of wave induced current drive by the combline antenna is the same. Therefore, the direction of the current seems to be determined by the pressure driven current. The large current modulation was correlated with the density modulation and that in the transmission power. Note that the combline antenna has an injection port, and waves propagate to the transmission port via mutual coupling between neighboring antenna elements. According to the cross correlation analysis, the change of the transmission power is about 0.2 ms delayed from the change in the current and the density. Therefore, the modulation of the transmission power is not the cause, but the result of the change in plasma. The fraction of the transmission power to the injected power is 10-20 %, indicating that a significant fraction of the power probably contributes to excite ling wave.

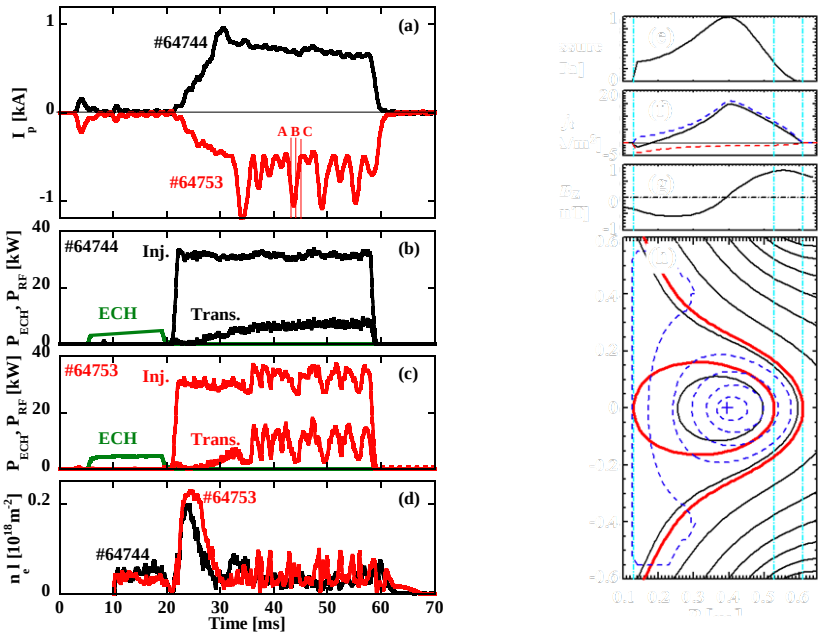

FIG. 3. Time evolution of the RF/combline start-up discharges with opposite external vertical field directions. Plasma current I_p (a), ECH power and net RF power at the injection and transmission ports (b) (c), and line integrated density (d). Reconstructed pressure profile (d), current density profile j_t (e), B_Z profile (f) and flux surfaces (g) at t = 50 ms for shot number #64744.

Figure 4 shows the time evolution of the equilibrium during a single oscillation (the timings A, B, C in FIG. 3(a)) of the plasma current. When the absolute value of the plasma current is increasing, the plasma has a similar profile to that of the low filling pressure ECH configuration, but the magnetic axis and the peak position of the current density are located at the inboard side. The peak position moves outward during the current peak. After that the value of the absolute plasma current decays, and the plasma stays near the outboard boundary, and a null point appears inside the vacuum vessel. It should be noted that inboard B_Z changes its polarity during a single oscillation. This large modulation causes a change in the antenna-plasma coupling, leading to a large modulation in the transmission power (FIG. 3(c))

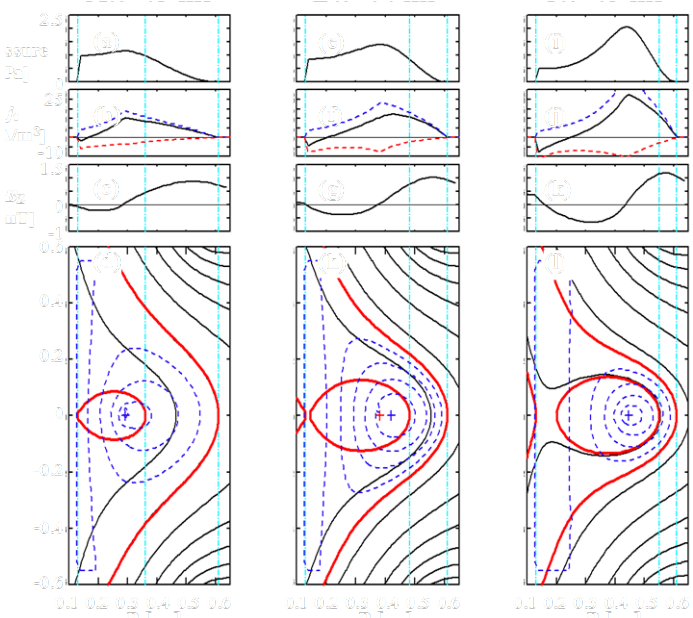

FIG. 4. Reconstructed pressure profile (a), (e), (i), current density profile j_t (b), (f), (j), B_Z profile (c), (g), (k) and flux surfaces (d), (h), (l) at three timings for shot number #64753 (see FIG. 3(a)).

The discharge duration for RF/single-strap and RF/combline is limited by the RF injection period. Although large current modulation appears in the counter-drive cases, the discharge duration is not affected. On the contrary, when we injected RF/HHFW (21 MHz), the sustained phase was often terminated by strong MHD activities [17].

3. Dependence of the plasma current on the external vertical field strength

It is obvious that the plasma current is roughly proportional to the external vertical field strength when ST plasma is in force equilibrium state. The relationship for ECH start-up plasmas was shown by many authors. Figure 5 summarizes the relationship for various heating scenarios. For ECH start-up discharges, the sustained current (after a current jump) increases with the external vertical field strength (closed rectangles). However, when the field strength exceeds a value, no current jump occurs, and the current stays at a low value (open rectangles). When we reverse the direction of the external vertical field, the same linear relationship was observed. For RF/single-strap start-up discharges, not only a linear relationship, but also the values are the same as those for ECH start-up discharges (closed triangles). In the case of RF/combline start-up discharges, a similar linear relationship was observed for the co-drive case. For the counter drive case, the current showed large

modulation. The peak value in the oscillation follows the same linear relationship as the ECH (solid line), but the bottom value in the oscillation is low. This feature suggests that the RF/combline start-up discharges take two stable states, one of which is the same state as ECH start-up discharge, and large oscillation represents a transition between the two states.

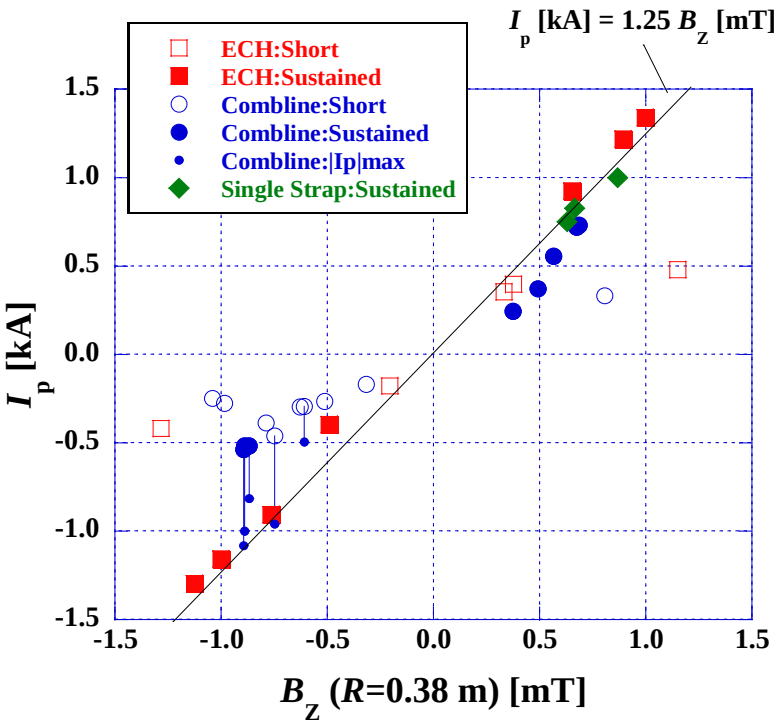

FIG. 7. Plasma current as a function of external vertical field strength. Various heating methods are plotted with different symbols. Closed symbols represent the values in the sustained phase after a current jump, open symbols represent the values for the discharges without a current jump.

Conclusions

Non-inductive plasma start-up experiments have been performed on the TST-2 spherical tokamak device using EC and RF power, and ST start-up and formation by RF wave in LH wave frequency range (200 MHz) were demonstrated for the first time. Equilibrium configurations of various operational scenarios were analyzed. Two types of configuration were found, and they seem to be determined by the fueling amount and the heating scenario. One has a center peaked current density profile and the other has a peak near the outboard boundary. With ECH, both types can be obtained depending on the filling pressure. On the other hand, only an outboard peaked current density profile was obtained by RF/single-strap. Center peaked current density profile was obtained also by the RF/combline scenario. These differences can be interpreted by different energy deposition profile. For RF/combline scenario, co-drive case and counter-drive case were compared. When the wave-induced current and the pressure driven current are parallel, we obtained a stable ST configuration similar to other scenarios. On the other hand, when they are anti-parallel, large current modulation appeared, and the phenomenon seems to represent a transition between two states.

Acknowledgments

This work was supported by Grants-in-Aid for Scientific Research (S) (21226021) and for Scientific Research (A) (21246137) of JSPS, Japan, and by National Institutes for Fusion Science NIFS10KOAR012.

References

[1] Mitarai, O., et al., J. Plasma Fusion Res. **80** (2004) 549.
[2] Nelson, B.A., et al., Phys. Rev. Lett. **72** (1994) 3666.
[3] Raman, R., et al., Nucl. Fusion **47** (2007) 792.
[4] Ono, M., et al., Phys. Rev. Lett. **59** (1987) 2165.
[5] Eidietis, N.W., et al, J. Fusion Energy **26** (2007) 43.
[6] Forest, C.B., et al., Phys. Rev. Lett. **68** (1992) 3559.
[7] Forest C.B. et al., Phys. Plasmas **1** (1994) 1568.
[8] Uchida, M., et al., J. Plasma Fusion Res. **80** (2004) 83.
[9] Yoshinaga, T., et al., J. Plasma Fusion Res. **81** (2005) 333.
[10] Maekawa, T., et al., Nucl. Fusion **45** (2005) 1439.
[11] Uchida, M., et al., Phys. Rev. Lett. 104 (2010) 065001.
[12] Ejiri, A., et al., Nucl. Fusion **46** (2006) 709.
[13] Kikukawa, T., et al. Plasma Fusion Res. **3** (2008) 010.
[14] Sugiyama, J., et al., Plasma Fusion Res. **3** (2008) 026.
[15] Shevchenko, V., et al., Nucl. Fusion **50** (2010) 022004.
[16] Watanabe, O., et al., Plasma Fusion Res. **3** (200) 049.
[17] Ejiri, A., et al., Nucl. Fusion **49** (2009) 065010.
[18] Takase, Y., et al., IAEA Fusion Energy Conference (Proc. 23rd Int. Conf. Daejon, 2010, FTP/P6-15).